# Kinematic Synthesis for 3D Signatures

Moises Diaz, Miguel A. Ferrer, Cristina Carmona-Duarte, Jose Juan Quintana,
Instituto Universitario para el Desarrollo Tecnológico y la Innovación en Comunicaciones (iDeTIC)
Universidad de Las Palmas de Gran Canaria, Spain
{moises.diaz, miguelangel.ferrer, cristina.carmona, josejuan.quintana}@ulpgc.es

Aythami Morales, Julian Fierrez
Biometrics and Data Pattern Analytics Lab
Universidad Autonoma de Madrid, Spain
{aythami.morales, julian.fierrez}@uam.es

Réjean Plamondon
École Polytechnique, University of Montreal, Montreal, QC, Canada.
rejean.plamondon@polymtl.ca

2022 IEEE International Joint Conference on Biometrics (IJCB) | 978-1-6654-6394-2/22/$31.00 ©2022 IEEE | DOI: 10.1109/IJCB54206.2022.10007945

## Abstract

*This paper proposes a method to generate the synthetic kinematic of signatures in 3D. The analysis of 3D signatures is becoming a hot topic due to the irruption of commercial off-the-shelf devices for easy acquisition of 3D movements. However, the novelty of this technology reveals the scarce publicly available signatures in 3D, which hinder their development. A solution is the synthesis of Signatures in 3D. As a first step, this paper synthesizes the kinematics of 3D signatures based on the Kinematic Theory of Rapid Movements and its associated Sigma-Lognormal model in 3D. To evaluate the method, we regenerate signature databases with synthetic speed profiles in all genuine and forgeries found in two 3D signature databases. Then, we analyze the similarities in the performance of a signature verifier when real and synthetic signatures are used in random and skilled forgeries experiments.*

## 1. Introduction

The synthesis of 2D signatures has promoted advances in the field of automatic signature verification. We observe this fact in offline (or static) and online (or dynamic) signatures because the synthesis can generate illimited data in both modalities [8]. Moreover, the extensive usage of signatures as legal evidence of authorship makes this trait very sensitive biometric data. Therefore, donating real signatures to public databases carries serious security concerns. As a solution, synthetic data allows researchers to share data without legal hindrances. This feasibility has opened the possibility of training and testing new automatic signature verifiers (e.g. [18]).

As part of the evolution of this technology, mainly boosted by the new commercial off-the-shelf (COTS) devices available for 3D movement acquisition, recent works have demonstrated the capacity to verify the authorship of signers through the 3D signatures in-air. Hence, it has direct applications in the biometric and e-security areas [16, 19].

As a recent verification modality, future designs in automatic signature verification in 3D may be more robust in case of a large quantity of available data. Because of that, all benefits supported by the synthesis of 2D signatures can be transferred to 3D signatures.

Furthermore, synthesizing such tridimensional movements opens the door to predicting movements, synthesizing human-like motions, and developing strategies for human motion reconstruction on engineered anthropomorphic systems, such as humanoids, mobile manipulators, and simulated systems.

The synthesis can be approached in two steps. On the one hand, generating complete artificial trajectories of signatures in 3D is required, and, on the other hand, the generation of kinematics. This paper focuses on the second generation as a preliminary step towards the full signature 3D synthetic generation.

One theory for analyzing the kinematics of human movement is the Kinematic Theory of Rapid Human Movements (e.g. [21, 22, 23, 24, 27]). This theory uses the Delta-Lognormal [25] and Sigma-Lognormal [20] models, which have been extensively used to explain most of the funda-

mental phenomena covered by classical studies on human motor control and to study several factors involved in fine motricity.

Two methods have been developed to work out the parameters with the Sigma-Lognormal model in 3D: ScriptStudio3D [12], which optimizes the velocity, and iDeLog3D (iterative Decomposition in Lognormals in 3D) [10], which optimizes the velocity and the trajectory jointly.

These methods transform 3D kinematic data into a sequence of circumference arcs between two virtual target points. Each arc is defined by starting and ending angles. An ending virtual target point is the starting virtual target point of the following circumference, and so on, up to the end of the movement. Similarly, each arc can be considered to have a starting and ending time, but the finishing time of an arc is not the same as the starting time of the next arc. Thus, the arcs are temporally overlapped. Each arc is covered with a lognormal velocity profile, and all the lognormal samples corresponding to the same time are summed to generate the trajectory. Consequently, the space-time trajectory is transformed into a sequence of virtual target points, starting and ending angles, and lognormal parameters. This analytical parametrization makes it easier to reverse the kinematic synthesis of signatures in 3D.

The kinematics synthesis for 3D signatures is practical in combination with the artificial generation of 3D trajectories. However, its independent use has also made sense on its own. Unstable frequency rates or bad quality in the timing signal and other noise because the acquisition devices render the deficient acquisition of the 3D movement. In some applications, a good kinematic estimator may substitute noisy original kinematics, which is generally obtained through processing the timing signal. The synthesis of the kinematics, used as a predictor, can help to improve the quality of the acquired samples. As a previous step to fully synthesizing 3D signatures, this paper studies kinematic generation. Note that many recognizers classify according to the kinematic properties of the signatures.

Based on these motivations and the kinematic parameters obtained with the Sigma-Lognormal Model in 3D [10], this work proposes a novel way to develop synthetic kinematics on tridimensional signatures. The main contributions of this work are twofold: *i*: we propose a novel 3D signatures biometric generation method capable of synthesizing human-like velocities in 3D genuine and forgery samples. The prerequisite to using the method is an 8-connected 3D trajectory without timing information. By using the order sequence of the ballistic trajectories in 3D, we developed a realistic kinematic for these movements in the frame of iDeLog3D [10]; *ii*: To evaluate the human likeness of the synthetic velocity, we compare the performance of real and synthetic databases[1] in experiments with an automatic signature verifier for 3D signatures [11]. The synthetic kinematic is finally validated according to random and skilled forgeries scenarios.

The rest of the paper is organized as follows. Section 2 details the method to synthesize the velocities in ballistic trajectories of signatures 3D. The evaluation is defined in Section 3 and the results are given in Section 4. We conclude the article in Section 5.

## 2. iDeLog3D for synthesis of kinematics in 3D trajectories

iDeLog3D is a model to represent the human kinematics with the Kinematic Theory of Rapid Human Movements and its associated Sigma-Lognormal model [10]. This model decomposed a human movement in 3D in a sum of temporally overlapped simple movements called strokes. In the kinematics synthesis, the strokes between two consecutive salient points in the trajectory will be found.

Then, each stroke has several parameters for its analytical representation. For the synthesis, we are estimating the lognormal timing, denoted by $t_{oj}$, the amplitude of the input command, $D_j$, the stroke time delay on a logarithmic scale, $\mu_j$, the stroke response time, $\sigma_j^2$, and the starting and ending angles, $(\theta_s, \theta_e)$, for each $j$ stroke. Note that the angles are two parameters do not require in the synthesis proposed in this paper.

In the following sections, we will describe the procedure in detail.

### 2.1. Linear interpolation and stroke segmentation in 3D

This section explains how the saleint points are computed from a 3D trajectory. Initially, the trajectory is sampled. From this real sampling, the real kinematic can be easily obtained. As we are interested in synthesized kinematics, we interpolated the sampling points in the $[x(t), y(t), z(t)]$ sequences with the Bresenham algorithm to create trajectories with eight connectivity. They can be expressed as $[x(i), y(i), z(i)]_{i=1}^{n}$, $n$ being the total number of points. We aim to develop the kinematic from these trajectories, which contain an ordered sequence of points.

The salient points in an 8-connected curve can be defined as the points with maxima curvature. They often coincide with the velocity profile minima due to the quick change of direction in the trajectory. In this way, the salient points of $[x(i), y(i), z(i)]$ are calculated as the peaks of the curvature, which is obtained at a point as [15]:

[1]The synthetic databases are publicly available for research purposes at `https://gpds.ulpgc.es/`.

$$\kappa(x,y,z)=\frac{\sqrt{\left(\ddot{z}\dot{y}-\ddot{y}\dot{z}\right)^2+\left(\ddot{x}\dot{z}-\ddot{z}\dot{x}\right)^2+\left(\ddot{y}\dot{x}-\ddot{x}\dot{y}\right)^2}}{\sqrt{\left(\dot{x}^2+\dot{y}^2+\dot{z}^2\right)^3}} \tag{1}$$

where $(\dot{x},\dot{y},\dot{z})$ are the differentiation of the sequence of $(x,y,z)$ Cartesian coordinates, respectively. The double upper dots denotes double differentiation. The radius of the curvature of a trajectory at a point $i$ in $[x(i),y(i),z(i)]$ is the inverse of the curvature $\kappa(x,y,z)$ at this point, $i$. Depending on how many samples we use for working out the differentiation, the curvature will be worked out at different scales.

In the practice, this procedure was not useful as many virtual target points were not located due to a big curvature in a plane, say plane $xy$, can be reduced in 3D owing to the trajectory in the orthogonal plane. To alleviate this drawback, the curvature in the plane $xy$ is calculated as:

$$\kappa(x,y)=\frac{\sqrt{\left(\ddot{y}\dot{x}-\ddot{x}\dot{y}\right)^2}}{\sqrt{\left(\dot{x}^2+\dot{y}^2\right)^3}} \tag{2}$$

similarly for the curvature in planes $xz$ and $yz$. The salient points in each plane are obtained as follows [7]: The curvatures at each plane are worked out at dozen scales uniformly distributed between 1 and $M/2$, $M$ being the length of the trajectory, and the scale the number of points used to work out the derivate. All the curvatures calculated are summed to obtain the summed curvature $C$. The salient points at each plane are selected as the peaks of $C$ whose height/width ratio are greater than $(\max(C)-\min(C))/45$. The salient points of the 3D trajectory are obtained as the union of the salient point of the $xy$, $xz$, and $yz$ planes [3].

Note that some salient points are detected in more than one plane $xy$, $xz$, or $yz$. However, as they are located in the same or nearby samples, they are combined in just one salient point. Figure 1 shows an example with the salient points initially detected during the analysis of two planes and the final salient points after their fusion with this method. Also, a detail in another view angle is shown.

Once selected the salient points, the starting timing reaction, the space, and the neuromuscular-based parameters are estimated.

## 2.2. Velocity profile synthesis

Given the sequence of salient points, $sp_j$, the velocity synthesis is based on a sum of lognormal functions inserted between consecutive salient points. There are many solutions to $t_{0j}, D_j, \mu_j$, and $\sigma_j^2$ fits the bell-shaped speed profile of a stroke [4]. According to the synergy of the neighbor

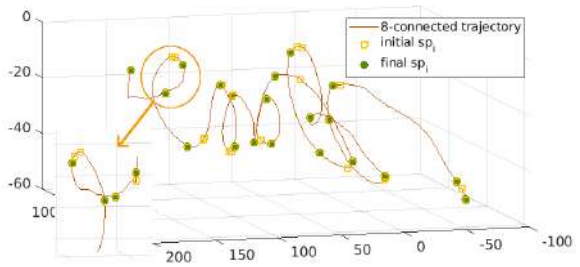


Figure 1: Example of initial and final salient points in a 8-connected 3D trajectory of signature and a detail.

lognormals studied by the kinematic theory, adjacent lognormals overlap to generate smooth and fluid movements.

Initially, a time is assigned to each salient point, $sp_j$. The salient points can be heuristically timed through this relation: $t_{0j}=ts_{j-1}-0.5$ [9], in seconds, giving enough time to the lognormal function to increase at the beginning of the stroke in $ts_{j-1}$.

To calculate $\mu_j$ and $\sigma_j^2$ parameters, we define a bell shape with a mean $M_j=ts_{j-1}+(ts_j-ts_{j-1})/2$ and variance $V_j=(ts_j-ts_{j-1})/4$ (it takes 95.45 % of energy in the segment and the rest of the overlap). This is an experimental value according to the general observations in the used databases of this article. Then the lognormal parameters are recovered by the method of moments [2]:

$$\begin{aligned}\mu_j&=\log\left(\frac{M_j^2}{\sqrt{V_j+M_j^2}}\right)\\ \sigma_j^2&=\log\left(\frac{V_j}{M_j^2+1}\right)\end{aligned} \tag{3}$$

and $D_j=l_{sj}$, where $l_{sj}$ is the distance between $sp_{j-1}$ and $sp_j$ in the 8-connected 3D trajectory.

Therefore, we define the velocity module as follows:

$$v(t)=\sum_{j=1}^{Nblog} D_j v_j(t) \tag{4}$$

$Nblog$ being the number of logormals and $v_j(t)$ is defined as:

$$v_j(t)=\frac{D_j}{\sigma_j\sqrt{2\pi}(t-t_{0,j})}\exp\left\{\frac{-\left[\ln(t-t_{0,j})-\mu_j\right]^2}{2\sigma_j^2}\right\} \tag{5}$$

## 2.3. Lognormal sampling of the 3D trajectory

Finally, the 3D 8-connected trajectory is sampled using the velocity module of Eq (4). To this end, a frequency of

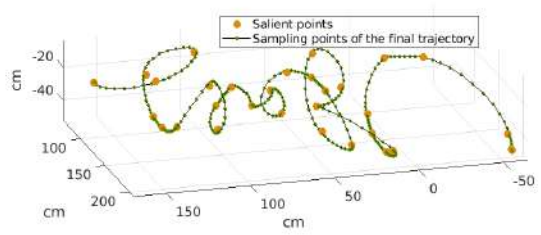


(a) Trajectory in 3D

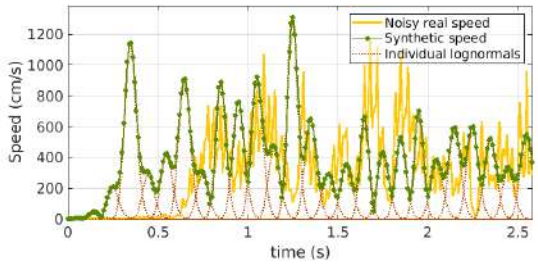


(b) Velocity

Figure 2: Example of a synthetic trajectory of a signature in 3D and a comparison between the noisy real and synthetic speeds on a 3D signature.

the output signal is assigned to mimick the samples per second, $f_m$, typically defined by the acquisition device. For example, let $k$ be a sampling point in the online 3D signatures and $k/f_m$ the timestamp of such sampling points, then the distance $d_k$ between samples in the 8-connected trajectory can be defined as follows:

$$d_k = \int_0^{k/f_m} v(t)\, dt \tag{6}$$

This distance, $d_k$, is later used to select the samples that satisfy the defined velocity profile, obtaining the online signature $(x(t), y(t), z(t))$.

Figure 2-a illustrated the sampled trajectory obtained from this procedure. To understand better the synthetic speed profile, Figure 2-b shows the real and synthetic speeds. As can be seen, the real profile is very noisy, including unrealistic high-frequency components that can only be explained as noise added by the acquisition device. Maybe, the noise origin is a non-uniform sampling frequency or location error. Instead, the synthetic speed is smoother according to the human muscular response. The number of lognormals of the synthetic speed relies on the number of salient points detected. In this way, a different number of salient points and different positions of the salient points render different speed profiles. Note that the aim is not to estimate the real speed profile but generate a realistic human-like speed that performs similarly to the real one.

As a detail, a practical null velocity was observed in the initial 0.5 s in the real speed (Figure 2-b). This hesitation time is tough to figure out, and our salient point estimator cannot estimate so many close salient points at the beginning of the signature. Despite not having the same speed profile as the real in a challenging case of 8-connected trajectories, we will validate their utility in automatic signature verification in the next sections.

## 3. Evaluation

To evaluate our method, we propose regenerating 3D signature databases with synthetic speed profiles and comparing the similarities between the performances obtained with the real and synthetic ones. Furthermore, the performance is obtained in automatic signature verification (ASV) experiments, a practical application of 3D signatures in e-security and robotic applications [16, 19]. In this way, The ASV is evaluated in different scenarios. Comparing the performance of a system when real or synthetic signatures are used is the most accepted evaluation in this field. However, other evaluations are convenient, like the perception of the signature.

### 3.1. Databases

The following publicly available databases of signatures in 3D were considered in this work.

- The 3DIIT Signatures database consists of 1600 air-written signatures by eighty individuals recorded using a Leap motion at 60Hz [1].
- The Deep3DSigAir database, which contains signatures from forty users: 10 for training, 10 for testing, and 25 forgeries acquired with Intel's creative senz3D depth camera at a sampling rate of 60Hz [19].

### 3.2. Forgeries in signature verification

We evaluate our synthesis method to reproduce human-like kinematics under the next two scenarios.

- Random Forgeries. This scenario consists of impersonating the user's identity with another personal signature. This experiment is relevant for its implications in e-commerce and similar transactions. In our case, we can simulate it with all databases.
- Skilled Forgeries. This is by far the most scathing attack on signature verification. It simulates a fake identity that has observed one or more than one signature of a genuine user. After learning and training for a while, the attacker tries to impersonate an enrolled user by imitating the signature maliciously. We do experiments with only the Deep3DSigAir, which provides skilled forgeries.

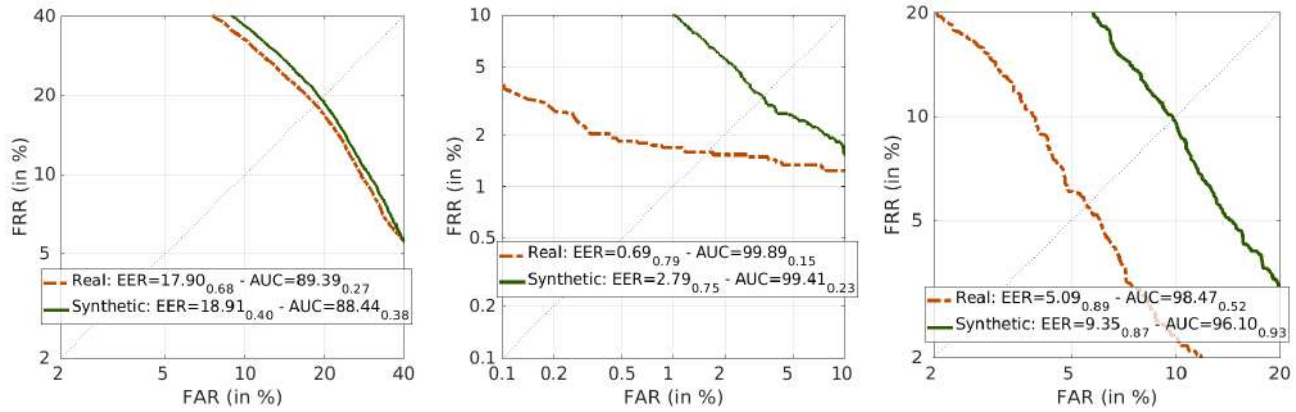


(a) Random forgery with 3DIIT (b) Random forgery with Deep3DSigAir (c) Skilled forgery with Deep3DSigAir

Figure 3: Random Forgery and Skilled Forgery results with the used signature databases in 3D.

Both scenarios serve to generate impostor scores. In addition, genuine scores are necessary to evaluate the performance of an ASV. Thus, genuine scores are produced when a legitimate user tries accessing the system using biometric data. Therefore, a 3D signature synthetic generation method must deal with these scores and their intra-class and inter-class distributions.

A new nomenclature for random and skilled forgeries was proposed in [14]. The authors recommended using bona fide attack and presentation attack, respectively. In addition, for this kind of test, similar vocabulary is proposed for the recent standard [17], which leads to the use of Attack Presentation Classification Error Rate (APCER) at fixed bona fide presentation classification error rate (BPCER) values.

Nevertheless, in this work, we prefer to preserve the well-known and accepted nomenclature of random and skilled forgeries. It can avoid confusion in the long term in automatic signature verification field [5, 26]. Moreover, the vocabulary does not introduce originality in the present research.

### 3.3. Protocol

To verify the signatures automatically, we use a dynamic time warping algorithm [11] using the trajectory and its first and second derivatives as features. In other words, it corresponds to the three coordinates of position, velocity, and acceleration, nine features in total. Then, the closer distance between a questioned signature and the enrolled set, normalized by the warping path length and the average distance among the enrolled set of signatures, was chosen as the final score.

We evaluate random and skilled forgeries experiments under classical metrics in biometrics. On the one hand, we worked out the False Rejection Rate (FRR) by comparing enrolled and genuine signatures. Then, the False Acceptation Rate (FAR) is built by comparing the identical enrolled signatures with forgeries.

Five random signatures were chosen as the enrolled set in all our experiments. The experiments were repeated ten times in all cases, and average Detection Error Tradeoff (DET) curves were given. We also reported the average threshold values of Equal Error Rate (EER) and Area Under Curve (AUC) and their standard deviations.

Both databases were used for the random forgery scenario. Per each user, we used all the genuine signatures not included in the enrolled set for developing the FRR curve. As forgeries, we use all genuine signatures of the other users for building the FAR curve.

For skilled forgeries, the same FRR curve was used. However, the FAR curve was built with all skilled forgeries available per each user in the Deep3DSigAir.

## 4. Results

### 4.1. Random forgery results

To validate the use of kinematics in random forgery, we compute the DET plots with real and synthetic signatures from the two databases. Figure 3-a and b show the performance with the 3DIIT and Deep3DSigAir databases, respectively.

We observe excellent results in the case of 3DIIT database. The real and synthetic curves are so close in all values of FAR and FRR in the logarithmic DET plot. Moreover, the EERs and AUCs between real and synthetic are close. In the case of Deep3DSigAir, we can see better closenesses in the DET curves in high FAR values.

We would like to highlight that we are not proposing an outperforming automatic signature verifier in 3D. Instead, we are using a standard system to analyze the similarities between the real and synthetic database performances, tested under the same conditions.

Table 1: Related works on synthesis of kinematics in signatures

| | **Real EER (%)** | **Synth. EER (%)** | **Database** |
|---|---|---|---|
| *Random forgeries* | | | |
| 2D signature: [6] | 0.71% | 0.88% | BiosecurID-132 [13] |
| 3D signature: *This work* | 17.90% | 18.91% | 3DIIT |
| 3D signature: *This work* | 0.69% | 2.79% | Deep3DSigAir |
| *Skilled forgeries* | | | |
| 2D signature: [6] | 5.46% | 9.51% | BiosecurID-132 [13] |
| 3D signature: *This work* | 5.09% | 9.35% | Deep3DSigAir |

### 4.2. Skilled forgery results

This case of skilled forgeries is the most challenging in signature verification. The performance comparison between real and synthetic is reported in Figure 3-c. Regarding the random forgery results with Deep3DSigAir databases, a positive effect of both DET curves is that they are parallel in the whole FAR and FRR ranges.

Finally, the results suggest that our generation method can produce realistic synthetic samples for different database conditions. The performance of the synthetic kinematics generated with the proposed approach varies from 0.69% to 17.90% of EER in Deep3DSigAir and 3DIIT databases, respectively (both for the same type of attack). It is worth pointing out that the proposed synthesizer can be adapted to the tendency of these performances in both random and skilled forgeries.

It is worth highlighting that this method can generate the kinematics of genuine and skilled forgeries. The input is just a 3D signature without temporal information. For this reason, experiments on random and skilled forgeries help to analyze the effectiveness of the kinematic generation.

### 4.3. Comparing with kinematic synthesis in 2D signatures

This research line has been active in 2D signatures. The Table 1 shows different works that have approached the kinematic of signatures in 2D for random and skilled forgeries. All works in this table used the same metrics and the same verifier. The objective of random and skilled forgeries experiments was to close the performance of the real database.

A fair comparison of 2D vs. 3D synthetic data would require using the same experimental protocol, ASV, and data. Probably, projecting the 3D signatures in 2D could be another practical solution for comparison. Nevertheless, the comparison results to [6] are certainly the first indications of the behavior of our synthesis.

In the case of random forgery, previous work reported similar relative performance errors. In our case, the 3DIIT performances are the most similar. However, in skilled forgeries, we can observe that our errors are in line with the previous works in 2D signature verification. Nevertheless, the comparison is not somewhat since the databases and experimental protocols were not the same.

Regarding the performances, detecting skilled forgeries with synthetic signatures in 2D and 3D rather than with reals seems more difficult. One reason is that the acquisition noise is not simulated with the biologically inspired computational model to synthesize the signatures. Another improvement aspect is the detection of the salient point in skilled forgeries. This detector works under the same conditions using genuine or skilled forgeries specimens, representing the most challenging case. Additionally, similar observations can be concluded in the case of random forgery. Finally, regarding the equal error rate values, the dependency on the database can be seen in Table 1, as usual in signature verification technology [5].

## 5. Conclusions

Motivated by the recent advance in automatic signature verification in 3D, we propose a method to synthesize the kinematic of signature trajectories in 3D. The kinematic synthesis is worked out under the lognormality principle of the Sigma-Lognormal model in 3D through iDeLog3D [10].

Our method starts from the 8-connected trajectory of the 3D signature. Firstly, we propose a method to estimate the salient points of the trajectory. Then, we define the strokes and their analytical parameters between these salient points. Finally, the trajectories are lognormally sampled to create a synthetic specimen for genuine and skilled forged 3D signatures.

We synthesized the signatures of two publicly available signature databases in 3D for validation. The results are put in context with the results obtained in similar approaches with signatures in 2D.

Our method neither increases the number of users in the databases nor the number of skilled forgeries. Instead, it designs artificially new velocity to a given 3D trajectory. Since our kinematic synthesis does not change the original signature trajectory, we cannot preserve private information.

We plan to design 3D synthetic trajectories of signatures in our future works. Then, we will investigate the integration of the kinematic synthesis proposed in this article. Moreover, the improvement of salient points estimation is still an open issue.

## 6. Acknowledgements

This study was funded by the Spanish government's MIMECO PID2019-109099RB-C41 research project and European Union FEDER program/funds, the CajaCanaria and la Caixa bank grant 2019SP19, and NSERC grant RGPIN-2015-06409.

## References

[1] S. K. Behera, D. P. Dogra, and P. P. Roy. Analysis of 3D signatures recorded using leap motion sensor. *Multimedia Tools and Applications*, 77(11):14029–14054, 2018.

[2] K. O. Bowman and L. Shenton. Estimation: Method of moments. *Encyclopedia of statistical sciences*, 3, 2004.

[3] C. De Stefano, G. Guadagno, and A. Marcelli. A saliency-based segmentation method for online cursive handwriting. *International Journal of Pattern Recognition and Artificial Intelligence*, 18(07):1139–1156, 2004.

[4] M. Diaz, M. A. Ferrer, C. Carmona, and R. Plamondon. Improving handwritten signatures fluency via the lognormality principle. In *The Lognormality principle and its applications in e-security, e-learning and e-health*, pages 41–63. World Scientific, 2021.

[5] M. Diaz, M. A. Ferrer, D. Impedovo, M. I. Malik, G. Pirlo, and R. Plamondon. A perspective analysis of handwritten signature technology. *ACM Computing Surveys (CSUR)*, 51(6):1–39, 2019.

[6] M. Ferrer, M. Diaz, C. Carmona-Duarte, and R. Plamondon. Improving on-line signature skillfulness. In *Workshop on Lognormality Principle and its Applications in Int. Conf. on Pattern Recogn. and Artificial Intel.*, pages 768–773, 2018.

[7] M. A. Ferrer, M. Diaz, and C. Carmona-Duarte. Two-steps perceptual important points estimator in 8-connected curves from handwritten signature. In *7th Int. Conf. on Image Processing Theory, Tools and Applications*, pages 1–5, 2017.

[8] M. A. Ferrer, M. Diaz, C. Carmona-Duarte, and A. Morales. A behavioral handwriting model for static and dynamic signature synthesis. *IEEE transactions on pattern analysis and machine intelligence*, 39(6):1041–1053, 2016.

[9] M. A. Ferrer, M. Diaz, C. Carmona-Duarte, and R. Plamondon. iDeLog: iterative dual spatial and kinematic extraction of sigma-lognormal parameters. *IEEE Transactions on Pattern Analysis and Machine Intelligence*, 42(1):114–125, 2020.

[10] M. A. Ferrer, M. Diaz, C. Carmona-Duarte, J. J. Quintana, and R. Plamondon. iDeLog3D: Sigma-lognormal analysis of 3dhuman movements. In *20th International Graphonomics Conference*, pages 1–15. Springer, 2022.

[11] A. Fischer, M. Diaz, R. Plamondon, and M. A. Ferrer. Robust score normalization for DTW-based on-line signature verification. In *13th Int. Conference on Document Analysis and Recognition (ICDAR)*, pages 241–245. IEEE, 2015.

[12] A. Fischer, R. Schindler, M. Bouillon, and R. Plamondon. Modeling 3D movements with the kinematic theory of rapid human movements. In *The Lognormality principle and its applications in e-security, e-learning and e-health*, pages 327–342. World Scientific, 2021.

[13] J. Galbally et al. On-line signature recognition through the combination of real dynamic data and synthetically generated static data. *Pattern Recogn.*, 48(9):2921–2934, 2015.

[14] J. Galbally, M. Gomez-Barrero, and A. Ross. Accuracy evaluation of handwritten signature verification: Rethinking the random-skilled forgeries dichotomy. In *IEEE International Joint Conference on Biometrics (IJCB)*, pages 302–310. IEEE, 2017.

[15] R. Goldman. Curvature formulas for implicit curves and surfaces. *Computer Aided Geometric Design*, 22(7):632–658, 2005.

[16] E. Guerra-Segura, A. Ortega-Pérez, and C. M. Travieso. In-air signature verification system using leap motion. *Expert Systems with Applications*, 165:113797, 2021.

[17] ISO Central Secretary. Information technology - Biometric presentation attack detection - Part 4: Profile for testing of mobile devices. Standard ISO/IEC 30107-4:2020, International Organization for Standardization, Geneva, CH, 2020.

[18] S. Lai and L. Jin. Recurrent adaptation networks for online signature verification. *IEEE Transactions on Information, Forensics and Security*, 14(6):1624–1637, 2018.

[19] J. Malik et al. Deepairsig: End-to-end deep learning based in-air signature verification. *IEEE Access*, 8:195832–195843, 2020.

[20] C. O'Reilly and R. Plamondon. Development of a sigma–lognormal representation for on-line signatures. *Pattern Recognition*, 42(12):3324–3337, 2009.

[21] R. Plamondon. A kinematic theory of rapid human movements: Part I. movement representation and generation. *Biological Cybernetics*, 72(4):295–307, 1995.

[22] R. Plamondon. A kinematic theory of rapid human movements. Part II. movement time and control. *Biological Cybernetics*, 72(4):309–320, 1995.

[23] R. Plamondon. A kinematic theory of rapid human movements: Part III. kinetic outcomes. *Biological Cybernetics*, 78(2):133–145, 1998.

[24] R. Plamondon, C. Feng, and A. Woch. A kinematic theory of rapid human movement. Part IV: a formal mathematical proof and new insights. *Biological Cybernetics*, 89(2):126–138, 2003.

[25] R. Plamondon and W. Guerfali. The generation of handwriting with delta-lognormal synergies. *Biological Cybernetics*, 78(2):119–132, 1998.

[26] R. Plamondon and G. Lorette. Automatic signature verification and writer identification—the state of the art. *Pattern recognition*, 22(2):107–131, 1989.

[27] R. Plamondon, C. O'reilly, J. Galbally, A. Almaksour, and É. Anquetil. Recent developments in the study of rapid human movements with the kinematic theory: Applications to handwriting and signature synthesis. *Pattern Recognition Letters*, 35:225–235, 2014.